

Non-trivial Infrared Structure in (2+1)-dimensional Quantum Electrodynamics

I.J.R. Aitchison , G. Amelino-Camelia, M. Klein-Kreisler[†], N.E. Mavromatos* and
D. Mc Neill

Department of Physics (Theoretical Physics), University of Oxford, 1 Keble Road, Oxford
OX1 3NP, U.K.

Abstract

We show that the gauge-fermion interaction in multiflavour $(2 + 1)$ -dimensional quantum electrodynamics with a finite infrared cut-off is responsible for non-fermi liquid behaviour in the infrared, in the sense of leading to the existence of a non-trivial fixed point at zero momentum, as well as to a significant slowing down of the running of the coupling at intermediate scales as compared with previous analyses on the subject. Both these features constitute deviations from fermi-liquid theory. Our discussion is based on the leading- $1/N$ resummed solution for the wave-function renormalization of the Schwinger-Dyson equations . The present work completes and confirms the expectations of an earlier work by two of the authors (I.J.R.A. and N.E.M.) on the non-trivial infrared structure of the theory.

[†]On leave from Instituto de Fisica, UNAM, Abdo. Postal 20-364, 01000 Mexico DF, Mexico.

*P.P.A.R.C. Advanced Fellow

July 1996

Recently two of us [1], in a paper from now on to be referred as I, have suggested that a Schwinger-Dyson (SD) analysis for the self-energy of the massless fermion of QED_3 provided intriguing evidence for a non-trivial infrared structure of the theory. We argued that the effective dimensionless running coupling constant varied slowly over a wide range of intermediate momenta lying between α (the mass scale of QED_3 , which plays the rôle of an ultra-violet cut-off [5]) and the infrared cut-off ϵ . This situation resembles that in (four-dimensional) ‘walking technicolour’ models of particle physics, and we described it in terms of a ‘quasi-fixed point’. The inclusion of wave-function renormalization was crucial to the effect. Equally important was the incorporation of a finite infrared cut-off.

This situation is very interesting from a condensed-matter point of view. There have been arguments [2] that a variant of QED_3 may serve as a continuum model for simulating the physics of the novel high-temperature superconductors. On the one hand, dynamical mass generation provides a mechanism for the spontaneous breaking of electromagnetic $U(1)$ symmetry, thus leading to superconductivity. On the other, deviations from trivial infrared fixed point structure have recently been argued to be responsible for departures from non-fermi liquid behaviour in the normal phase [3, 1] in which no dynamical mass is generated. Indeed the presence of wave-function renormalization yields marginal $O(1/N)$ -corrections to the ‘bulk’ non-fermi liquid behaviour caused by the gauge interaction in the limit of infinite flavour number $N \rightarrow \infty$. Such corrections lead to the appearance of modified critical exponents. In particular, at low temperatures there appear to be logarithmic scaling violations of the linear resistivity of the system of order $O(1/N)$ [1].

In I we based our arguments on an approximate form of the leading- $1/N$ resummed SD equations, which was an improved version of the results of ref. [4]. The approximation employed in [4] was strictly valid for a regime of momenta $p \ll \alpha$, while that in [1] was appropriate to $p \simeq \alpha$. For the actual physical models, however, the regime of momenta over which deviations from fermi liquid behaviour is observed is much wider than those employed in ref. [4] or ref. [1]. To extend the validity of the arguments of I over a wider momentum regime in a mathematically rigorous way one needs to have a more precise picture of the situation by employing as exact expressions for the $O(1/N)$ SD equations as possible. In particular we would like to re-examine the way the effective coupling constant runs in the momentum range $0 < p < \alpha$, in a regime of parameters such that there is no dynamical mass generation. That is the purpose of this note. As we shall see, the situation is exactly as predicted by the preliminary approximate analysis of I, thereby confirming the expectations of that reference.

To this end, it seems instructive first to recapitulate the arguments of I while briefly reviewing the formalism. The SD equations, in the one-loop resummed $1/N$ limit, read

$$A(p) = 1 - \frac{\alpha}{\pi^2 N} \frac{1}{p^3} \int_0^\infty dk \frac{k A(k) G(p^2, k^2)}{k^2 A(k)^2 + B(k)^2} I(p, k), \quad (1)$$

where

$$I(p, k) \equiv \alpha^2 \ln \frac{p+k+\alpha}{|p-k|+\alpha} - \alpha(p+k-|p-k|) + 2pk -$$

$$\frac{1}{\alpha}|p^2 - k^2|(p + k - |p - k|) - \frac{1}{\alpha^2}(p^2 - k^2)^2 \left\{ \ln \frac{p + k + \alpha}{|p - k| + \alpha} - \ln \frac{p + k}{|p - k|} \right\}, \quad (2)$$

and

$$B(p) = \frac{\alpha}{\pi^2 N} \frac{1}{p} \int_0^\infty dk \frac{k B(k) G(p^2, k^2)}{k^2 A(k)^2 + B(k)^2} \left\{ 4 \ln \frac{p + k + \alpha}{|p - k| + \alpha} \right\} \quad (3)$$

where the Landau gauge has been assumed, and $\alpha \equiv \frac{e^2 N}{8}$ is the dynamically-generated scale of the theory. $A(p)$ is the wave-function renormalization, $B(p)$ is the mass-gap function, and $G(p^2, k^2)$ is a vertex function. The integrals in (1) and (3) are effectively cut-off at α , due to a sharp decay of the integrands above this scale [5]. Hence α may be considered as an effective UV cut-off. Moreover, for reasons that will become clear below we also introduce an infrared cut-off ϵ . Following ref. [4], we make the vertex ansatz

$$\Gamma_\mu(p^2, k^2) = \gamma_\mu A(k)^n \equiv \gamma_\mu G(k^2). \quad (4)$$

The Pennington and Webb [6] ansatz corresponds to $n = 1$, where chiral symmetry breaking occurs for arbitrarily large N [7]. It is this case that was argued to be consistent with the Ward identities that follow from gauge invariance [6]. Here we shall concentrate on the $n = 1$ ansatz. It is interesting to note from (1),(3) that in this case the right hand sides of the SD equations depend only on the ratio $B(p)/A(p) \equiv \Sigma(p)$, which is the physical gap function.

For the purposes of I, and of this note, we are interested in the normal phase of the theory where the mass gap $B(p)$, or equivalently $\Sigma(p)$, can be ignored in the denominators of (1). In that case, equation (1) for $A(p)$ reduces to simple quadrature if $n = 1$. Using the ansatz (4), one can then analyze the Schwinger-Dyson (SD) equations, in the various regimes of momenta, in terms of a running coupling obtained from substituting the solution for $A(p)$ into equation (3) for the gap:

$$g_R(p, \epsilon) = \frac{g_0}{A(p, \epsilon)} \quad (5)$$

where $g_0 = 8/\pi^2 N$, N is the number of fermion flavours, and ϵ is an infrared cutoff. The reader might have wondered whether the definition (5) of a running coupling makes any sense in the normal phase of the model, where dynamical mass generation is absent. The resolution of this comes from treating the gap equation (3) as a non-trivial equation, of which the vanishing gap appears as a consistent solution. This provides a definition of g_R which continues smoothly from the phase of dynamical mass generation to the normal phase. Furthermore, the definition (5) of the running coupling is also justified within the conventional framework of Gell-Mann-Low renormalization of the gauge model.

The following two approximations were suggested in ref. [4]:

$$\begin{aligned} \ln \frac{p + k + \alpha}{|p - k| + \alpha} &\simeq 2 \left\{ \frac{k}{p + \alpha} + \frac{1}{3} \left(\frac{k}{p + \alpha} \right)^3 + \dots \right\} \Theta(p - k) + \\ &2 \left\{ \frac{p}{k + \alpha} + \frac{1}{3} \left(\frac{p}{k + \alpha} \right)^3 + \dots \right\} \Theta(k - p) \end{aligned} \quad (6)$$

and

$$\begin{aligned} \ln \frac{p+k+\alpha}{|p-k|+\alpha} &\simeq 2\left\{\frac{k}{\alpha} - \frac{kp}{\alpha^2} + \frac{3pk^2+k^3}{3\alpha^3}\right\}\Theta(p-k) + \\ &2\left\{\frac{p}{\alpha} - \frac{pk}{\alpha^2} + \frac{3pk^2+p^3}{3\alpha^3}\right\}\Theta(k-p). \end{aligned} \quad (7)$$

Using (7), and neglecting $B(k)$ in the denominator of (1), the following approximate form for $A(p)$ in (1) may then be derived [4]

$$A(p) = 1 - \frac{g_0}{3} \int_{\epsilon}^{\alpha} dk \frac{G(k^2)}{kA(k)} \left\{ \left(\frac{k}{p}\right)^3 \Theta(p-k) + \Theta(k-p) \right\}. \quad (8)$$

Note that the form of the infrared regulator, which has now been introduced explicitly, is—following [4]—simply a momentum-space cut-off. In [4] an approximate expression for g_R was given which was based on (8), but with the further approximation of retaining only the term with $\Theta(k-p)$, while neglecting the one involving $\Theta(p-k)$. This produces the result (always for $n=1$ in (4))

$$\begin{aligned} g_R^{KN} &= \frac{g_0}{1 + \frac{g_0}{3} \ln(p/\alpha)} && \text{for } \epsilon < p < \alpha \\ &= \frac{g_0}{1 + \frac{g_0}{3} \ln(\epsilon/\alpha)} && \text{for } 0 < p < \epsilon. \end{aligned} \quad (9)$$

In I, by contrast, the term $\Theta(p-k)$ in (8) was retained and the one with $\Theta(k-p)$ was dropped, leading to

$$g_R^{AM} = \frac{g_0}{1 - \frac{g_0}{9} + \frac{g_0}{9} (\epsilon/p)^3}, \quad (10)$$

an approximation which was argued to be valid for $p \simeq \alpha$. Whereas g_R^{KN} grows as p decreases, g_R^{AM} exhibits the opposite behaviour, and this was interpreted in I as indicating that the true dependence of g_R on p/α would be significantly slower than that of g_R^{KN} - a situation we described in terms of a ‘quasi fixed point structure’.

It is clearly important to establish the extent to which the conclusions drawn from (9) or (10) are in fact reliable. Of course, a numerical solution of (1) and (3) is always possible (see below), but more insight can often be gained from analytical results, provided they are not artefacts of a too-crude approximation scheme. In both I and [4] the authors were interested in exploring the effects of different n 's in (4). But, as stated above, the case $n=1$ seems the most relevant. The main purpose of the present note is to exploit the simplifications associated with the $n=1$ case to investigate more rigorously the issues raised in I and [4].

Before embarking on the calculations, we remark that for simplicity we shall present results only for one value of N (or g_0). We select the number of flavours N to lie comfortably in the regime where dynamical mass is not generated. From the analysis of [4] and [8] it becomes clear that there is a critical number of flavours for dynamical mass generation to occur, and that this

depends on the infrared cut-off. Although at present we have not studied the corresponding critical line in any detail, we can be sure that the value $N = 5$ will exceed the critical line for the regime of infrared cut-offs that are physically interesting to us [1], i.e. $10^{-3} < \delta/\alpha < 10^{-1}$. We shall present results for the value $N = 5$.

The simplest improvement of I and [4] is obviously to retain both Θ terms in (8). We easily find (for $n = 1$)

$$g_R^{(8)} = g_0/A^{(8)}(p, \epsilon) \quad (11)$$

with

$$\begin{aligned} A^{(8)} &= 1 - \frac{g_0}{9} + \frac{g_0}{9} \left(\frac{\epsilon}{p}\right)^3 + \frac{g_0}{3} \ln\left(\frac{p}{\alpha}\right) \quad \text{for } \epsilon < p < \alpha \\ &= 1 + \frac{g_0}{3} \ln\left(\frac{\epsilon}{\alpha}\right) \quad \text{for } 0 < p < \epsilon \end{aligned} \quad (12)$$

which is simply the obvious combination of (9) and (10). The quantities $g_R^{(8)}$ and g_R^{KN} are shown in figure 1, from which we see that, as compared with (9), (12) provides essentially a smooth approach to the region $0 \leq p \leq \epsilon$ where g_R is constant (in this approximation). In this region, there is a line of non-trivial infrared fixed points, corresponding to the value $g_R^* = g_0/(1 + \frac{g_0}{3} \ln(\epsilon/\alpha))$. By demanding positivity of $A^{(8)}(p, \epsilon)$ at $p = \epsilon$ one can obtain a mild restriction on ϵ :

$$\epsilon \geq e^{-\frac{3}{g_0}} \alpha \quad (13)$$

which is reasonable for $g_0 \ll 1$.

The existence of a non-trivial infrared fixed point was one of the main conjectures of I, relevant for the non-fermi liquid behaviour of the system. Actually the same structure is evident in the $n = 1$ curve of figure 1 of [4], though it was not remarked upon there; a similar conjecture was also made previously for four-dimensional *QCD* in ref. [9]. The second conjecture made in I, also implying a non-fermi liquid behaviour, pertains to a significant slowing down of the rate of decrease of g_R with increasing p at intermediate scales of momenta, relative to that shown by g_R^{KN} . Such behaviour is not apparent from figure 1; indeed, $g_R^{(8)}$ and g_R^{KN} run essentially parallel until p is quite close to ϵ . However, the conjectured behaviour at intermediate values of p will in fact emerge from the more accurate treatment which now follows. As we shall see, the restriction (13) also disappears, and one gets a non-trivial infrared fixed point structure at $p = 0$.

In order to improve upon (11), we return to (1) with $B = 0$, $n = 1$, and a momentum-space cut-off ϵ . The running of the coupling $g_R(p, \epsilon)$ is then defined by (5) with

$$A(p, \epsilon) = 1 - \frac{\alpha}{\pi^2 N} \frac{1}{p^3} \int_{\epsilon}^{\infty} \frac{dk}{k} I(p, k) \quad (14)$$

which we have evaluated numerically. The resulting $g_R(p, \epsilon)$ is also shown in figure 1, for comparison with $g_R^{(8)}$ and g_R^{KN} . It is indeed apparent that the exactly evaluated $g_R(p, \epsilon)$ does run significantly more slowly than either of the approximate quantities $g_R^{(8)}$ and g_R^{KN} , thus confirming the second conjecture of I.

In the discussion thus far, we have implemented the infrared regularization by a simple momentum-space cut-off ϵ . It may be questioned whether it is consistent, in this case, to consider values of the external momentum p lying below ϵ , as we have done in figure 1. Indeed, the behaviour of $g_R(p, \epsilon)$ for p near ϵ and below it is, in our view, unlikely to be physical. Detailed examination shows that dg_R/dp vanishes at $p^* = \epsilon(1 + \mathcal{O}[\epsilon/\alpha])$, where g_R reaches a maximum. However, for smaller values of the external momenta there is a decrease of g_R towards $p = \epsilon$, so that p^* is not a fixed point. For values of p less than ϵ , g_R decreases further, leading ultimately (it appears) to a fixed point at $p = 0$. This behaviour seems unphysical, and may signal an inconsistency between the vertex ansatz of (4) and the momentum-space cut-off scheme, at small momenta. We would like to find an infrared regularization in which both p and the integration variable k could range between 0 and α , and which would be expected to lead to smoother results, for small p , than those of figure 1. Besides, it is important to check whether the main qualitative features of our results are independent of the details of the infrared regularization scheme.

Fortunately, there is a consistent way of implementing the infrared cut-off within the ansatz (4), which satisfies these criteria. We keep the limits of integration from 0 to α , and interpret the mass function B/A in (1) as a (covariant) infrared cut-off in the case of no dynamical mass generation. The expression for A then reads

$$A(p, \delta) = 1 - \frac{\alpha}{\pi^2 N} \frac{1}{p^3} \int_0^\alpha dk \frac{k}{k^2 + \delta^2} I(p, k), \quad (15)$$

and the associated coupling $g_R(p, \delta)$ is defined by $g_R(p, \delta) = g_0/A(p, \delta)$. This way of introducing the infrared (IR) cut-off makes some contact with the finite temperature case [1, 8], where the plasmon mass was interpreted as an effective infrared cut-off. The above similarity is, however, only indicative. Whether the situation described here carries over intact to the finite-temperature regime is at present only an expectation. These are issues that are left open for future investigations.

We may now repeat, for the “ δ ” cut-off case, the calculations described above for the “ ϵ ” cut-off. We first consider the use of (7) in (15), with the further restriction of keeping only the $\Theta(k - p)$ term, as in [4]. This gives

$$g_R^{KN, \delta} = \frac{g_0}{1 + \frac{g_0}{6} \ln \frac{p^2 + \delta^2}{\alpha^2 + \delta^2}}, \quad (16)$$

which agrees with (9) for $p > \epsilon$ as $\delta \rightarrow 0$, and provides a smooth continuation to $p = 0$. Next, we retain both Θ terms, as in (8), leading to

$$g_R^{(8), \delta} = g_0/A^{(8)}(p, \delta) \quad (17)$$

where (c.f. (12))

$$A^{(8)}(p, \delta) = 1 - \frac{g_0}{9} + \frac{g_0}{3p^2} \delta^2 - \frac{g_0}{3p^3} \delta^3 \arctan\left(\frac{p}{\delta}\right) + \frac{g_0}{6} \ln\left(\frac{p^2 + \delta^2}{\alpha^2 + \delta^2}\right). \quad (18)$$

Again we note that for fixed δ (18) goes smoothly to a constant value as $p \rightarrow 0$. Finally, we calculate $g_R(p, \delta)$ numerically.

The results are shown in figure 2, which may be compared directly with figure 1. The first observation is that the appearance of the three curves is qualitatively very similar in the “ ϵ ” and “ δ ” cases, confirming that the detailed form of the infrared cut-off is not making a qualitative difference. Secondly, one sees that $g_R^{(8),\delta}$ runs parallel to $g_R^{KN,\delta}$ until p is near δ , and that both these approximations give significantly faster running than the exact $g_R(p, \delta)$. Finally, we stress that there is a non-trivial fixed point at $p = 0$, which is approached perfectly smoothly, in contrast to the unusual behaviour shown in figure 1. The result for $g_R(p, \delta)$ is therefore in full agreement with the expectations of I regarding a ‘walking technicolour’-like behaviour of g_R at intermediate scales of momenta.

To emphasize the insensitivity of these results to the form of the infrared cut-off, we show again in figure 3(a) the curves $g_R(p, \epsilon)$ of figure 1 and $g_R(p, \delta)$ of figure 2, for $\epsilon = 0.5$ and $\delta = 0.5$. Of course, there is no reason why such a comparison has to be made at the same numerical values of ϵ and δ , and we could have adjusted one of them to get closer matching of the results. But this would contain no extra physics: figure 3(a) already shows convincingly enough that the two crucial elements—the non-trivial fixed point at $p = 0$ and the slow running—are independent of the form of the cut-off.

It is interesting to note that the above features are characteristic of the presence of a *finite* infrared cut-off. Removal of δ via $\delta \rightarrow 0$ in a smooth manner does not seem to be possible, as becomes clear from figure 3(b). From a physical point of view [1], where the infrared cut-off is conjectured to be associated with temperature in certain condensed-matter systems whose physics the above model is supposed to simulate, this would imply that the above non-trivial structure is an exclusive feature of the finite-temperature field theory.

We add one final comment on the various approximations introduced above. Our exact numerical results based on either (14) or (15) show that the attractively simple formula (8) (or the analogous one with the δ cut-off), which requires *both* of the approximations (6) and (7), fails to capture the slow running at intermediate momenta. However, approximation (6) alone does appear to be sound, and worth pursuing further. The expression for A based on (6), with the δ cut-off, is

$$A^{(6)}(p, \delta) = 1 - \frac{\alpha}{\pi^2 N} \frac{1}{p^3} \int_0^\alpha dk \frac{k}{k^2 + \delta^2} \{f(p, k) + f(k, p)\} \quad (19)$$

where

$$f(p, k) = \frac{2k^3(4\alpha^3 p^3 + 4\alpha^2 p^4 + \alpha^2 p^2 k^2 - 3p^4 k^2 + \alpha^2 k^4 + 3\alpha p k^4 + 3p^2 k^4)}{(3\alpha(\alpha p + p^2))^3} \Theta(p - k), \quad (20)$$

and we define the corresponding g_R by $g_R^{(6)} = g_0/A^{(6)}(p, \delta)$. The integrals in (19) can be performed analytically, with the result:

$$A^{(6)}(p, \delta) = 1 - g_0 \left\{ \frac{p^3}{12 \alpha \delta^2} - \frac{p^4}{12 \alpha^2 \delta^2} + \frac{p^2 (2 \alpha^2 - p^2)}{96 \alpha^2 (\alpha^2 + \delta^2)} - \frac{p^2 (2 \alpha^2 - p^2)}{24 (\alpha^2 + \delta^2) (\alpha + p)^2} + \right.$$

$$\begin{aligned}
& \frac{(p - \alpha) (4\alpha^6 + 4\alpha^4 \delta^2 - 2\alpha^4 p^2 - 6\alpha^2 \delta^2 p^2 - \alpha^2 p^4 + \delta^2 p^4)}{24\alpha (\alpha^2 + \delta^2)^2 (\alpha + p)} + \\
& \frac{140\alpha^2 \delta^4 p^2 - 105\alpha^2 \delta^6 - 315\alpha \delta^6 p - 315\delta^6 p^2 - 420\alpha^3 \delta^2 p^3 + 105\alpha \delta^4 p^3}{1260 p^5 (\alpha + p)^3} + \\
& \frac{140\alpha^3 p^5 - 476\alpha^2 \delta^2 p^4 - 210\delta^4 p^4 - 63\alpha \delta^2 p^5 + 176\alpha^2 p^6 + 42\delta^2 p^6 + 45\alpha p^7 - 18p^8}{1260 p^5 (\alpha + p)^3} + \\
& \frac{\delta^3 (\alpha^2 \delta^4 + 3\alpha \delta^4 p - \alpha^2 \delta^2 p^2 + 3\delta^4 p^2 + 4\alpha^3 p^3 + 4\alpha^2 p^4 + 3\delta^2 p^4)}{12 p^6 (\alpha + p)^3} \arctan\left(\frac{p}{\delta}\right) + \\
& \frac{8\alpha^5 \delta^4 + 8\alpha^3 \delta^6 + \alpha^5 \delta^2 p^2 - 9\alpha \delta^6 p^2 - \alpha^5 p^4 - 3\alpha^3 \delta^2 p^4 - 6\alpha \delta^4 p^4}{12 \delta^3 (\alpha^2 + \delta^2)^3} \left(\arctan\left(\frac{\alpha}{\delta}\right) - \arctan\left(\frac{p}{\delta}\right) \right) + \\
& \frac{4\alpha^2 \delta^4 - 4\alpha^6 + 3\alpha^4 p^2 + 8\alpha^2 \delta^2 p^2 - 3\delta^4 p^2 + \alpha^2 p^4 - 3\delta^2 p^4}{24 (\alpha^2 + \delta^2)^3} \ln\left(\frac{4\alpha^2 (\delta^2 + p^2)}{(\alpha^2 + \delta^2) (\alpha + p)^2}\right) \} \quad (21)
\end{aligned}$$

The interesting point is that $g_R^{(6)}(p, \delta)$ turns out to be almost indistinguishable from the exact $g_R(p, \delta)$, showing that (6) is actually very reliable. This is shown in figure 4. The availability of this very accurate analytical expression for g_R might be useful. For example, taking the derivative of (21) with respect to p it is straightforward to show that the non-trivial infrared fixed point does lie at $p = 0$. It is probably of interest to the detailed reader to note that the more crude approximation consisting of keeping only the $\Theta(k - p)$ terms in (6), which is an improved version of what was done in [4], exhibits a much better agreement with the exact answer of fig. 2 and (21) than that based on the approximation (9). This shows that the inadequacy of the approximation of ref. [4] lies mainly in the steps leading to (7), rather than in the neglect of modes with momentum below p .

To conclude, in this short note we have solved the SD equations (1), with the ansatz $n = 1$ in (4), for the wave-function renormalization in the normal phase of the model, where dynamical mass is ignored. The solution has been exact, in the sense that it is valid for a wide region of momenta $0 < p < \alpha$. The solution indicated that the increase of the running coupling is cut-off in the infrared, in the form of a non-trivial fixed point, and that there is also a significant slowing down of the running of the coupling at intermediate scales, as compared to the case of ref. [4] or of Eq. (11). This slowing down, or ‘walking-technicolour-like’ behaviour, has been argued [1] to be responsible for the smallness of the coherence length of the dynamical-mass-generation phase of the theory. On the other hand, both features, the non-trivial infrared structure and the walking-coupling behaviour at intermediate scales, have been argued in I to be responsible for deviations from fermi-liquid behaviour, which might have important physical consequences, in case the model simulates correctly the physics of the novel high-temperature superconductors. We have also argued that the above non-trivial low-energy structure is a consequence of a *finite* infrared cut-off. Thus, from the physical point of view, adopted in I, of associating the infrared cut-off with temperature effects, this would imply that the above

structure is an exclusive feature of the finite-temperature field theory.

Acknowledgements

We would like to acknowledge discussions with L. Del Debbio, S. Hands, and K. Kondo. G.A.-C. acknowledges financial support from the European Union under contract #ERBCH-BGCT940685. M.K.-K. thanks the Royal Society of London and the Mexican Academy of Scientific Research (AIC), under a joint collaboration programme, for supporting financially a visit to the University of Oxford, during which the present work was carried out. D.McN. wishes to thank PPARC for a research studentship.

References

- [1] I.J.R. Aitchison and N.E. Mavromatos, Phys. Rev. B 53 (1996), 9321..
- [2] N. Dorey and N.E. Mavromatos, Phys. Lett. B250 (1990), 107; Nucl. Phys. B386 (1992), 614.
- [3] R. Shankar, Physica A177 (1991), 530; Rev. Mod. Phys. 66 (1994), 129.
- [4] K. Kondo and H. Nakatani, Progr. Theor. Phys. 87 (1992), 193.
- [5] T. Appelquist, M. Bowick, D. Karabali and L.C.R. Wijewardhana, Phys. Rev. D33 (1986), 3704;
T. Appelquist, D. Nash and L.C.R. Wijewardhana, Phys. Rev. Lett. 60 (1988), 2575.
- [6] M.R. Pennington and S.P. Webb, BNL Report No. BNL-40886 (1988) (unpublished);
M.R. Pennington and D. Walsh, Phys. Lett. B253 (1991), 246;
D.C. Curtis, M.R. Pennington and D. Walsh, Phys. Lett. B295 (1992), 313.
- [7] R.D. Pisarski, Phys. Rev. D29 (1984), 2423.
- [8] I.J.R. Aitchison and M. Klein-Kreisler, Phys. Rev. D50 (1994), 1068.
- [9] K. Higashijima, Phys. Rev. D29 (1984), 1228.

Figure Captions

Figure 1: Running coupling constant of large- N resummed QED_3 in the normal phase as a function of the external momenta p , in the presence of a momentum-space infrared cut-off ϵ . In the figure $\epsilon = 0.1$, $\alpha = 1$, and $N = 5$; the dotted curve shows g_R^{KN} of (9); the top continuous curve shows $g_R^{(8)}$ of (11) and (12); the bottom continuous curve shows the exact (numerical) result, $g_R(p, \epsilon)$.

Figure 2: As in figure 1, but now employing a covariant infrared-mass cut-off $\delta = 0.1$. The dotted curve is $g_R^{KN, \delta}$ of (16); the top continuous curve is $g_R^{(8), \delta}$ of (17); the bottom continuous curve is $g_R(p, \delta)$.

Figure 3: A comparative study of the running of the QED_3 coupling in the cases with momentum-space (ϵ) and covariant-mass (δ) infrared cut-offs for $\alpha = 1$, $N = 5$. In (a) the dotted and continuous curves show $g_R(p, \epsilon = 0.1)$ and $g_R(p, \delta = 0.1)$ respectively. In (b) is shown the value of the coupling $g_R(p = x, x)$ at momenta of order of the generic infrared cut-off x , as a function of the cut-off (the dotted curve corresponds to the ϵ cut-off, whilst the continuous one corresponds to the δ cut-off). Clearly the cut-off cannot be removed smoothly in either case.

Figure 4: Test of the validity of the analytic result (21), based on the approximation (6), in the covariant mass-cut-off δ case. The running of the coupling based on (21) (dotted curve) is compared with the exact numerical result (continuous curve), for $\alpha = 1$, $\delta = 0.1$ and $N = 5$. The agreement is very good throughout the entire range of external momenta $0 < p < 1$.

FIGURE 1

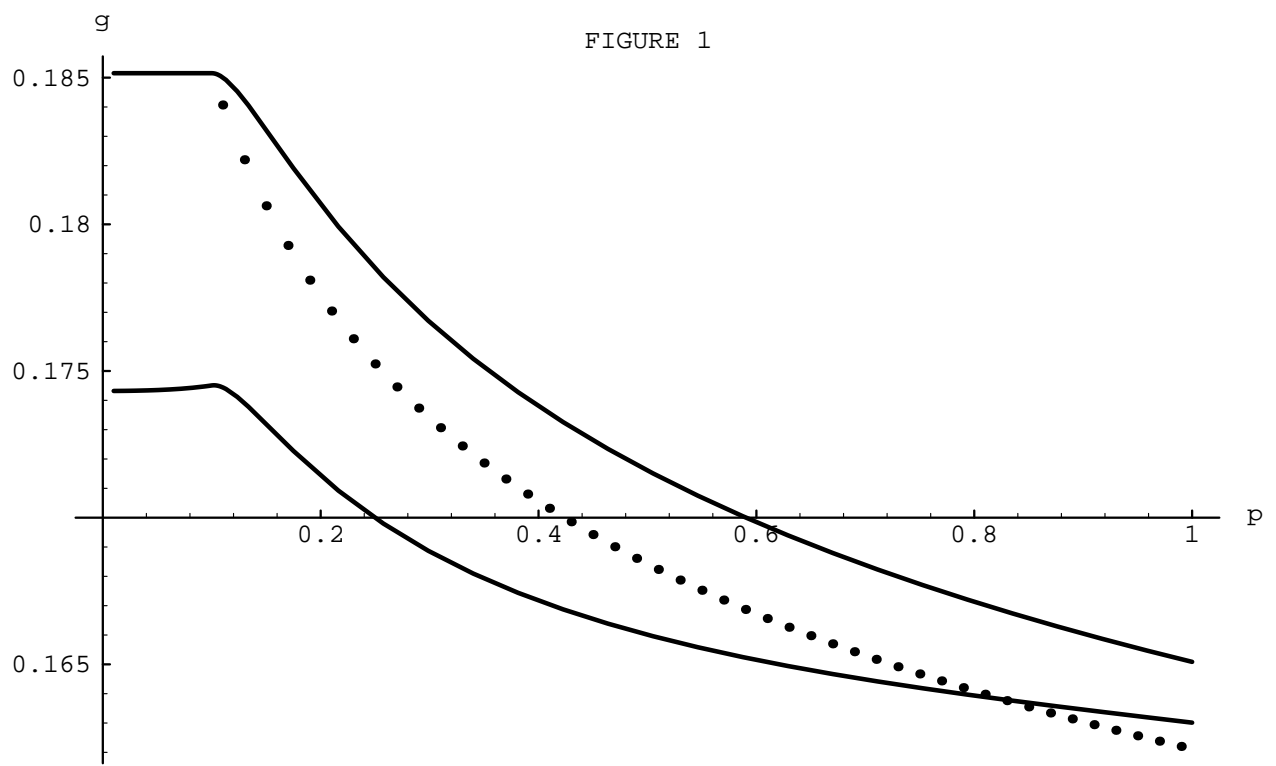


FIGURE 2

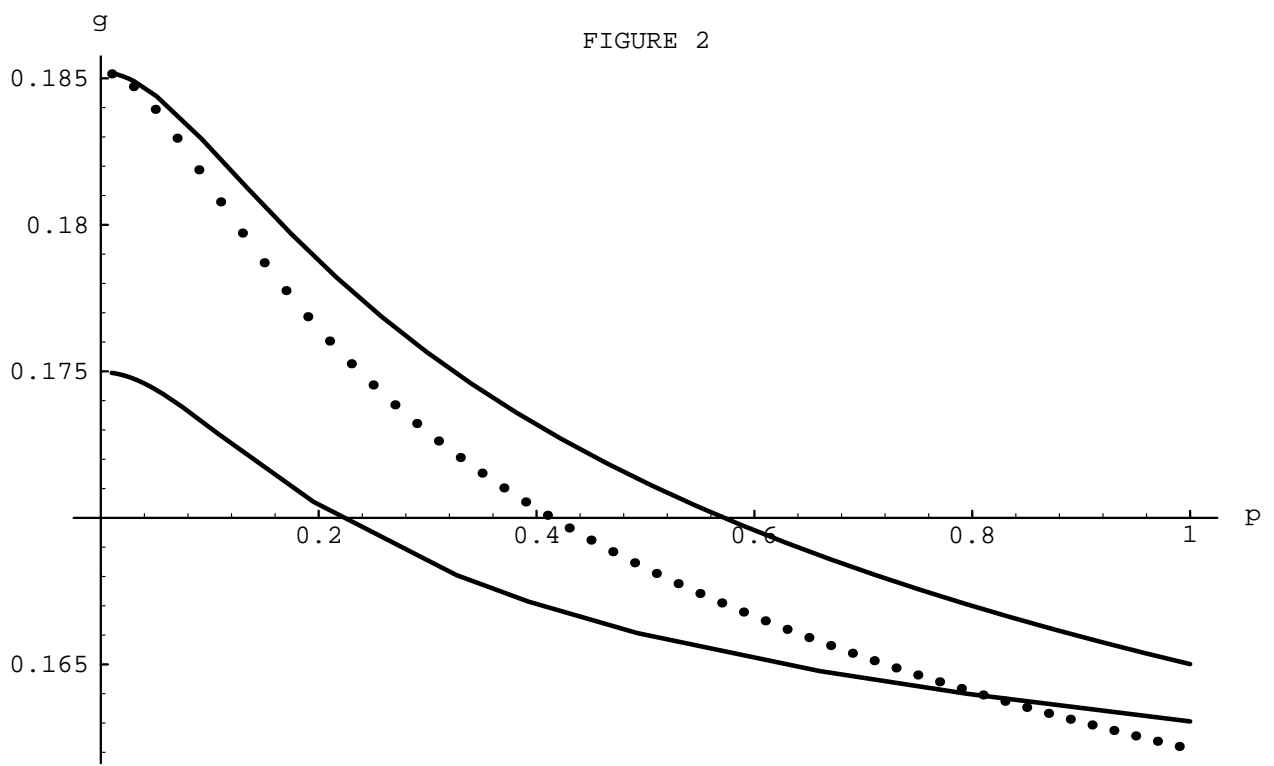


FIGURE 3a

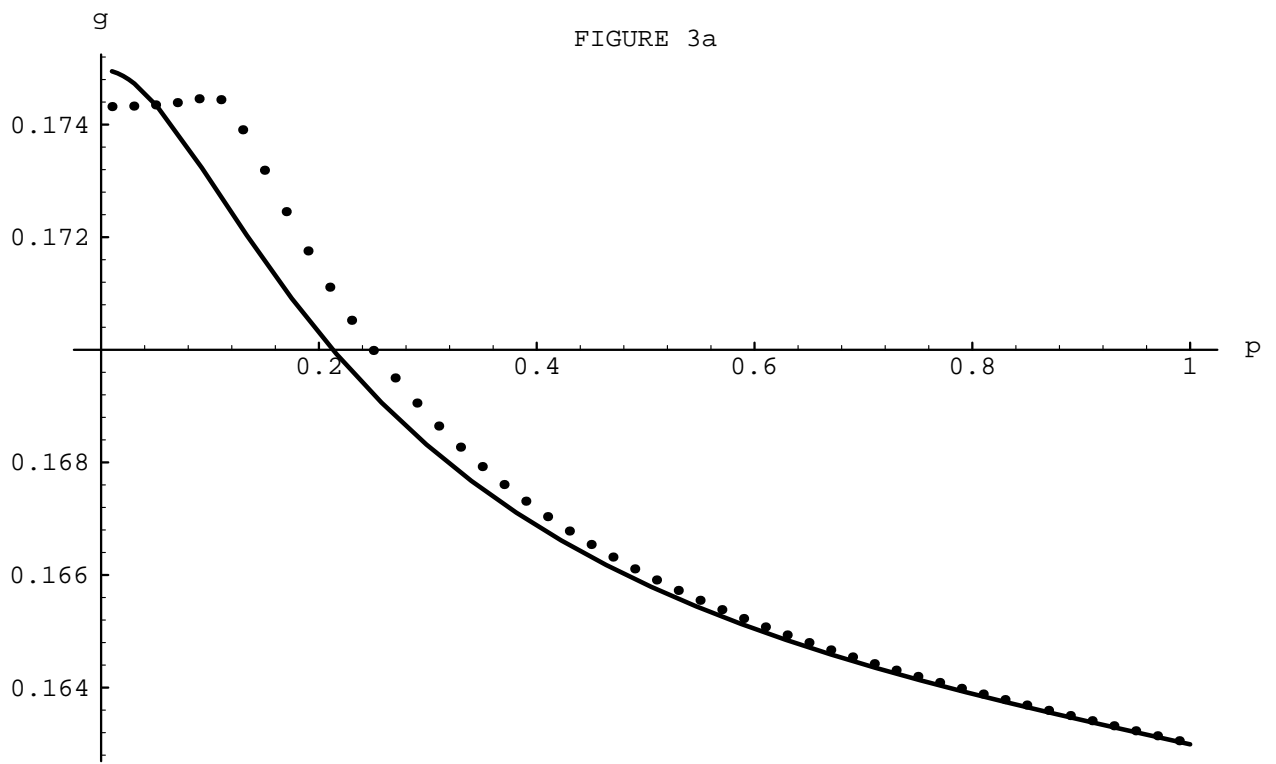


FIGURE 3b

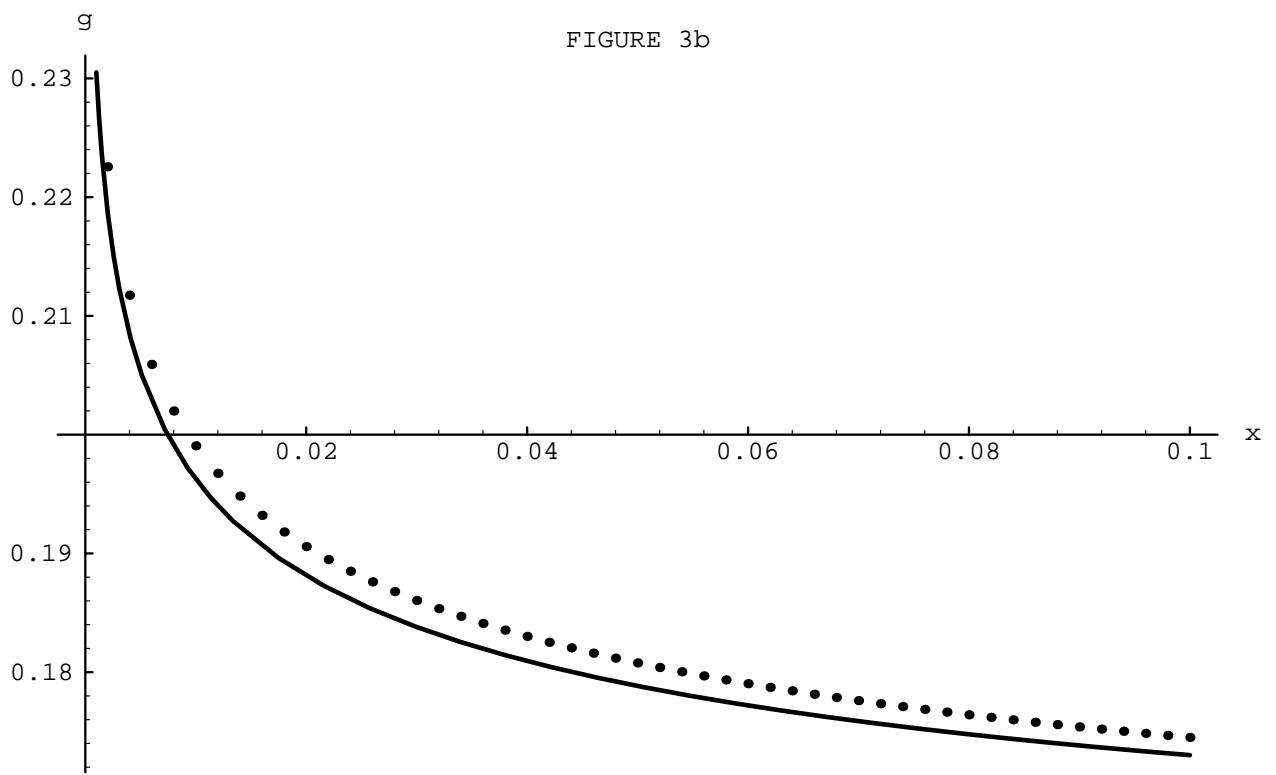


FIGURE 4

